Further insight into the gas flame acceleration mechanisms in pipes. Part II : numerical work

Guillaume Lecocq, Emmanuel Leprette, Jérôme Daubech, Christophe Proust

Further insight into the gas flame acceleration mechanisms in pipes. Part II: numerical work

Guillaume Lecocq [a], Emmanuel Leprette [a], Jérôme Daubech[a] & Christophe Proust[a,b]

E-mail: *Guillaume.lecocq@ineris.fr*

[a] Institut National de l'Environnement Industriel et des Risques, Parc Technologique ALATA, BP 2, 60550 Verneuil-en-Halatte, France
[b] Sorbonne Universités, UTC-TIMR, 1 rue Dr Schweitzer, 60200 Compiègne, France

Abstract

This paper is the second part of a global work investigating the physics of premixed flame propagation in several kinds of long pipes. It focuses on the potential of CFD for modelling such cases and on the key issues for being able to address generic cases. Four tests among the database detailed in the first part are selected. In each case, the pipe is straight, open at one end and closed at the other where ignition is triggered. The pipe is filled with a stoichiometric methane/air mixture at rest. Varied parameters are the inner pipe diameter and the pipe material.

CFD computations, based on a URANS framework were carried out and enabled to recover several physical trends, such as the role of acoustics and boundary layer turbulence on the flame dynamics. Although most overpressure peaks orders of magnitude of the measured overpressure signals can be predicted numerically, the computed flames are quicker than the measured ones. It could be explained by the chosen turbulent model, the k-ω SST model, known to be adapted for wall-bounded flows but producing too much turbulence for accelerating flows. The criterion for the near wall cells ($y^+<200$) might be too loose as well.
Keywords: *premixed flame, methane, pipe, CFD*

1. Introduction

Recent works (Daubech, 2018) enabled to measure pressure signals and flame speed histories for a set deflagrations occurring in long straight pipes with an open end for varying diameters and materials. These tests highlight the influence of :

- The acoustics at least in smooth pipes ;
- the nature of the pipe and potentially the influence of the roughness of the wall on the flow.

The oscillatory behaviour of flames propagating in long pipes was previously observed (Guénoche, 1964, Kerampran, 2000) and recovered with models assuming one-dimensional flames and small propagation speed compared to the speed of sound (Fachini, 2013).

Nevertheless, to the author's knowledge, no single "engineer" model was already proven to be able to predict all the trends mentioned above. It is a challenge as such models are deduced simplifying the full set of equations theoretically describing the deflagration. In this process, effects influencing the flame dynamics such as the three-dimensional topology, the impact of geometrical details and coupling between physical phenomena can be easily lost.

CFD is attractive for providing a general model as it can account for all the required physics, given the proper modelling choices are made.

Turbulence in particular can be addressed in several ways in the codes: it can be totally resolved by some lab codes (Moureau, 2011), modelled with the RANS/URANS frameworks as it has been done for many years for industrial designs (Cornejo, 2018) or partially resolved with LES (Urbano, 2017) which is an increasing trend. Mixed RANS/LES techniques were also proposed (Makowka, 2017). For each framework, several combustion models were proposed by the scientific community. Nevertheless, even if more resolution of the physics is the most attractive method for the modeller, it implies more computing power, which is a limited resource.

To the author's knowledge, deflagrations in long pipes with no obstacles were rarely investigated with CFD. Such configurations are among the most challenging premixed flame modelling cases as the flame is not stabilized, implying all the proper phenomena to be properly modelled at each instant for recovering experimental flame histories.

The current paper aims at providing the industrial risk engineer new elements to contribute to answer to the following questions:

- It is possible to recover with CFD the experimental flame speed history and pressure signals for such cases?
- What could be the accuracy of CFD?
- What is the price to pay by the modeller for getting accurate results? A higher resolution of the physics by the grid, implying more computational power? Or proper modelling choices for turbulence and/or combustion among the bibliography?

In this goal, the paper first describes the identified set of experiments, then the adopted modelling strategy and finally details the comparison of the predicted flame speeds and overpressure signals with the measured ones.

2. Cases of interest

The paper focuses on some experiments described in the parent paper (Daubech, 2018). In each case, the pipe is straight, 24-m long, open at one end and closed at the other. It is filled with a quiescent stoichiometric methane/air mixture. Ignition is performed on the middle of the closed end with an electrical spark whose energy is about 100 mJ.

Four tests are modelled, for varying pipe inner diameter and material. These tests, as well as the methods employed for measuring pressure and flame speed are summed up in the Table below. Figure 1 shows some of the studied pipes.

Table 1: Selected pipe deflagration tests.

Inner diameter	Material	Pressure probe locations (from ignition point)	Flame tracking method (distances are considered from ignition point)
250 mm	PMMA	0 m, 5 m, 15.5 m	High-speed camera and video processing
	Steel	0 m, 5.4 m, 15.8 m	Photovoltaic cells at: 1.5 m, 8.1 m, 11.9 m and 19.7 m
150 mm	PMMA	0 m, 5.4 m, 15.5 m	High-speed camera and video processing
	Steel	0 m, 5 m, 15.5 m	Photovoltaic cells at: 0.5 m, 5.5 m, 10.5 m and 15.5 m

These tests are attractive as methane/flames are quite easy to model compared with other hydrocarbons or hydrogen as the tendency of self-instabilities production related to non-unitary Lewis number effect is moderate. The geometry is also simple, enabling to rely on a high-quality mesh, reducing the impact of numerics. Furthermore, the sensibility of two parameters from a reference case is studied

Figure 1: View of the experimental set-up. Top: PMMA pipe, with a 250-mm inner diameter. Bottom: metal pipe, with a 150-mm inner diameter.

3. Modelling strategy

3.1 Physical models

The CFD model has to account for a premixed flame whose propagating speed may not satisfy low Mach number assumptions and can be driven by acoustics, flow curvature and turbulence generation at the walls. For the sake of simplicity, a URANS approach is chosen for modelling turbulence. Indeed, performing a proper LES is more demanding on the mesh as a large part of the turbulent energy should be resolved by the grid (Pope, 2004).

The Favre-averaged transport equations of pressure, momentum, energy, chemical species and progress variable are solved numerically by the OpenFoam code (Weller, 1998), version 3.0.0. The solver is compressible and solve the acoustics.

Turbulence is modelled with the k- ω SST model (Menter, 2003), commonly adopted for wall-bounded flows. A known drawback of this model nevertheless is it can produce large turbulence levels in regions with strong accelerations (Fouladi, 2015), which is potentially the case for the flames propagating in pipes.

The chemistry is addressed with a one-step reaction and only methane, oxygen, nitrogen, carbon dioxide and water mass fractions are transported.

Turbulent premixed flame can be modelled with a flame surface-density ($\bar{\Sigma}$) approach. This quantity is approximated as $\Xi|\nabla\tilde{c}|$, where Ξ is the wrinkling factor of the flame related to flame/turbulence interaction and $\tilde{c}$ is the Fabre-averaged progress variable. The chemical source terms of the Favre-averaged progress variable and chemical species mass fractions can be closed as (Lecocq, 2011):

$$\bar{\rho}\widetilde{\dot{\omega}_c} = \rho_u S_L \Xi |\nabla\tilde{c}|$$

$$\bar{\rho}\widetilde{\dot{\omega}_{Y_i}} = \bar{\rho}\widetilde{\dot{\omega}_c}(Y_i^b - Y_i^u)$$

Where ρ_u is the volume mass of the fresh gases, $S_L$is the laminar flame speed, Y_i^b (resp. Y_i^u) is the burned (resp. fresh) gases mass fraction of the i-th chemical species.

The wrinkling factor of the flame is closed algebraically as:

$$\Xi = 1 + \left(1 + 2\Xi_{shape}(c - 0.5)\right)\Xi_{coeff}\sqrt{\frac{u'}{S_L}}R_\eta$$

Where Ξ_{shape} and Ξ_{coeff} are parameters set to 1 and 0.2, c is the progress variable, u' is the fluctuating speed and R_η equals $u'/\left(\epsilon\tau_\eta\right)^{0,5}$ where ϵ is the turbulence dissipation rate. ${\tau_\eta}^2 = (\nu/\rho_u\epsilon)$ with ν, the kinematic viscosity. It was checked before CFD runs (not shown) that the correlation for Ξ gave satisfying results when compared with experiments in which turbulence interacts with methane/air flames (Liu, 2012).

3.2 Computational domain and grid

The computational domain is limited to the part of the pipe filled by the flammable mixture. At walls, velocity is zero and turbulent viscosity is modelled with a wall law. At the outlet plane, the pressure is set to the atmospheric pressure and the velocity gradient is set to 0.

In all cases, the thermal impact of the material is neglected and walls are assumed to be adiabatic (pressure gradient set to 0). The PMMA is assumed perfectly smooth and the steel roughness is assumed to be around 150 μm which corresponds to a weakly rusted steel. The turbulent boundary layer is theoretically divided into three parts: a viscous sub-layer close to the wall, an intermediate buffer sub-layer and a logarithmic sub-layer. This latter can be modelled with the following equation: $u^+ = 1/\kappa \ln(Ey^+)$ that relates u^+ and y^+, the normalized flow velocity and distance to the closest wall. κ is the Von Karman constant (0.41) and E is a constant set to 9.8. The previous equation is valid for smooth walls only. In OpenFoam, another boundary condition is proposed for rough walls. It relies on a shift of the log law with E depending on the wall roughness.

Different grids are used, each one being characterized by a number of cells. For each pipe, the reference mesh is made of 1.4 million cells. A fine mesh is made of 2.5 million cells. A very fine mesh for the 150-(resp. 250-) mm pipe contains 4.3 (resp. 6.0) million cells. All grids are composed of hexahedra only, with a characteristic size decreasing from pipe centre to the walls.

The computations are performed for a given case with the reference mesh. The logarithmic sub-layer assumption is valid for values of y^+ ranging roughly between 30 and 200. If this criterion is not fulfilled during the flame propagation, especially if $y^+ > 200$ during the flame acceleration, a finer grid is used for a new computation of the case.

3.3 Computing resources

The computations were run in parallel on several cores of a supercomputer. The computations times were about 10 hours for 1s of physical time with 256 2.4 GHz Intel Xeon cores

4. Results

4.1 250-mm pipes

4.1.1 The PMMA pipe

A classic way to study flame propagation is to plot the flame position versus time diagram. The numerical flame position is the distance on the pipe axis between the close end and the point where the progress variable equals 0.5.

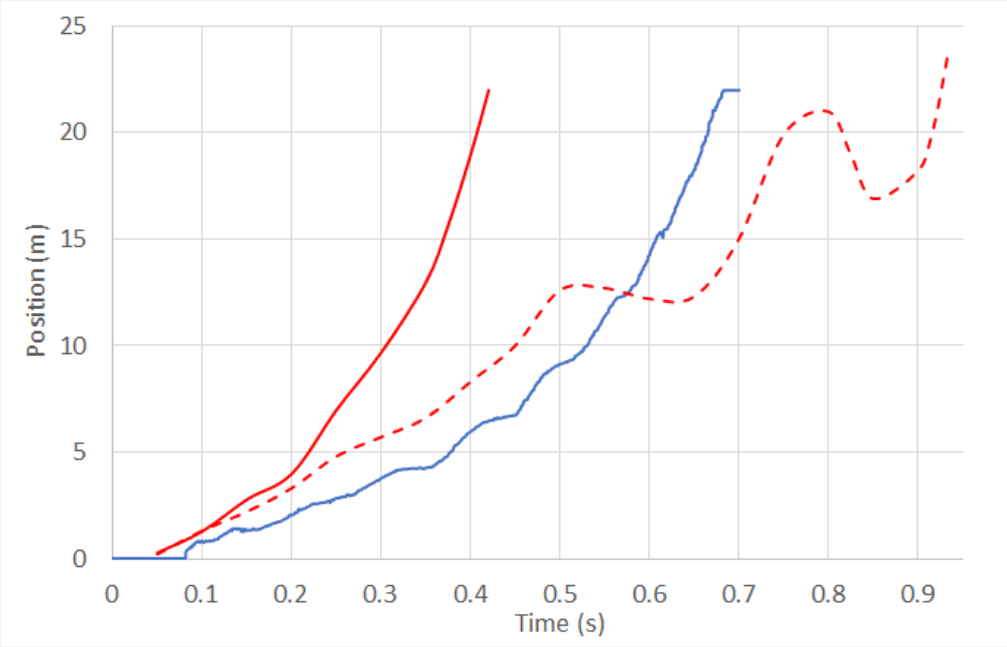

Figure 2: History of the flame front position obtained from the video post-processing (blue), the computations with (red straight line) and without (red dotted line) a modelled turbulence.

The comparison between histories of flame positions (Figure 2) shows a numerical flame that propagates on average about 60% quicker than the measured one and not accounting for oscillatory behaviour. Another computation was performed with no modelled turbulence and Ξ set to 1 to investigate these gaps. The laminar and the turbulent numerical flames propagate at the same speed from 0 to 0.2 s, which is too high compared to the experiment. It could be partly explained by the chemical model: the burnt gases temperature in the code is about 2600 K, whereas theoretical adiabatic flame temperature at constant pressure is about 2230 K, according to a Gaseq computation (Morley, 2005). Such a gap indeed leads to an overestimation of the expansion rate of the burnt gases which in turn artificially boosts the flame speed. The overestimation is about 20 %. A solution could be to add species like H_2 and CO in the burnt gases composition to improve the temperature prediction.

At a time of about 0.2 s, the turbulent flame strongly accelerates whereas the average speed of the laminar flame is roughly the same from 0 to 0.55 s and follows the experimental trend. The laminar flame shows an oscillatory behaviour but the period seems to be about 0.2 s, greater than the experimental period about 0.08 s. From 0.55 s to the end of the laminar flame propagation, the flame goes backwards whereas the experimental flame keeps on moving forward.

Figure 3 details the laminar flame evolution with time. The modelled flame is never purely flat. It is first elongated (0.5 and 0.1 s) and then adopts a tulip shape (from 0.15 to 0.25 s). It is interesting to note such phenomenon can be recovered whereas its origin is still a discussion topic in the scientific community (Xiao, 2012). The time needed for an acoustic wave to propagate from the flame front to the open end and to come back is about 0.15 s. The shape change thus appears directly related to flame/acoustics interaction. From 0.25 s to the end of flame propagation, the flame shape changes constantly, switching from a tulip to an elongated shape with characteristic periods. Note the flame shape directly impacts the flame propagation speed because the total fresh gases consumption rate increases with the flame surface. For the

turbulent flame (not shown), flame shapes changes occur during the combustion of a third of the pipe length and for the rest of the propagation, the flame remains elongated. It seems to mean the flame is sensible to acoustics when it is sufficiently slow.

After 0.5 s, the laminar flame model is no more coherent with experiment. It may be explained by an impact more and more pronounced of turbulence on the flame as the flame approaches the pipe end, that is not accounted by the model and/or by the decreasing distance between the outlet boundary condition and the flame front. Extra computations should be performed meshing a part of the atmosphere and moving the boundary conditions away from the flame path.

It appears CFD can approach with a laminar assumption for half the flame propagation length. When turbulence is accounted for, the model predicts an overestimated production rate and/or amount although the walls are assumed to be smooth. It can be due to the turbulence model itself and/or to the criterion on the maximum value of y^+ which could be not constraining enough.

It should be noted that according to the experiment interpretation (Daubech, 2018), turbulence may not play such an important role in the flame propagation history contrary to other phenomena like acoustics. This observation explains why the best numerical agreement is obtained with the laminar flame assumption.

The computed and measured overpressure signal 15.5 m from ignition point are shown in Figure 4. In coherence with observations from the flame histories, the best results are obtained with the laminar model, in terms or order of magnitudes for overpressures and characteristic periods from 0 to 0.45 s. After this time, the coherence is lost. It is noticeable that even if the turbulent flame propagates too quickly compared to the experiment, the characteristic orders of magnitude for the overpressures are predicted. It is maybe due to a balance between a higher pressure production by the flame inducing an enhanced volume flow rate at the outlet plane.

4.1.2 The metal pipe

The turbulent flame model is tested for the metal pipe case.

Figure 5 shows the effect of rugosity on the results: from 0 to about 0.2 s, the flame propagation speed for a smooth and a rough pipe are similar and after 0.2 s, the rough pipe flame propagates faster. Again, turbulence seems to be produced too quickly when compared to the experiment. Nevertheless, the quantitative impact of roughness on the average flame speed seems to be recovered by CFD with an increase of about 20 %.

Figure 6 highlights the model predicts the periods about 0.2 s of the experimental overpressure signal despite the overpressure peaks are overestimated. Even for flames which seem to be predominantly driven by flame/turbulence interactions, acoustics still play an important role on the overpressure signal.

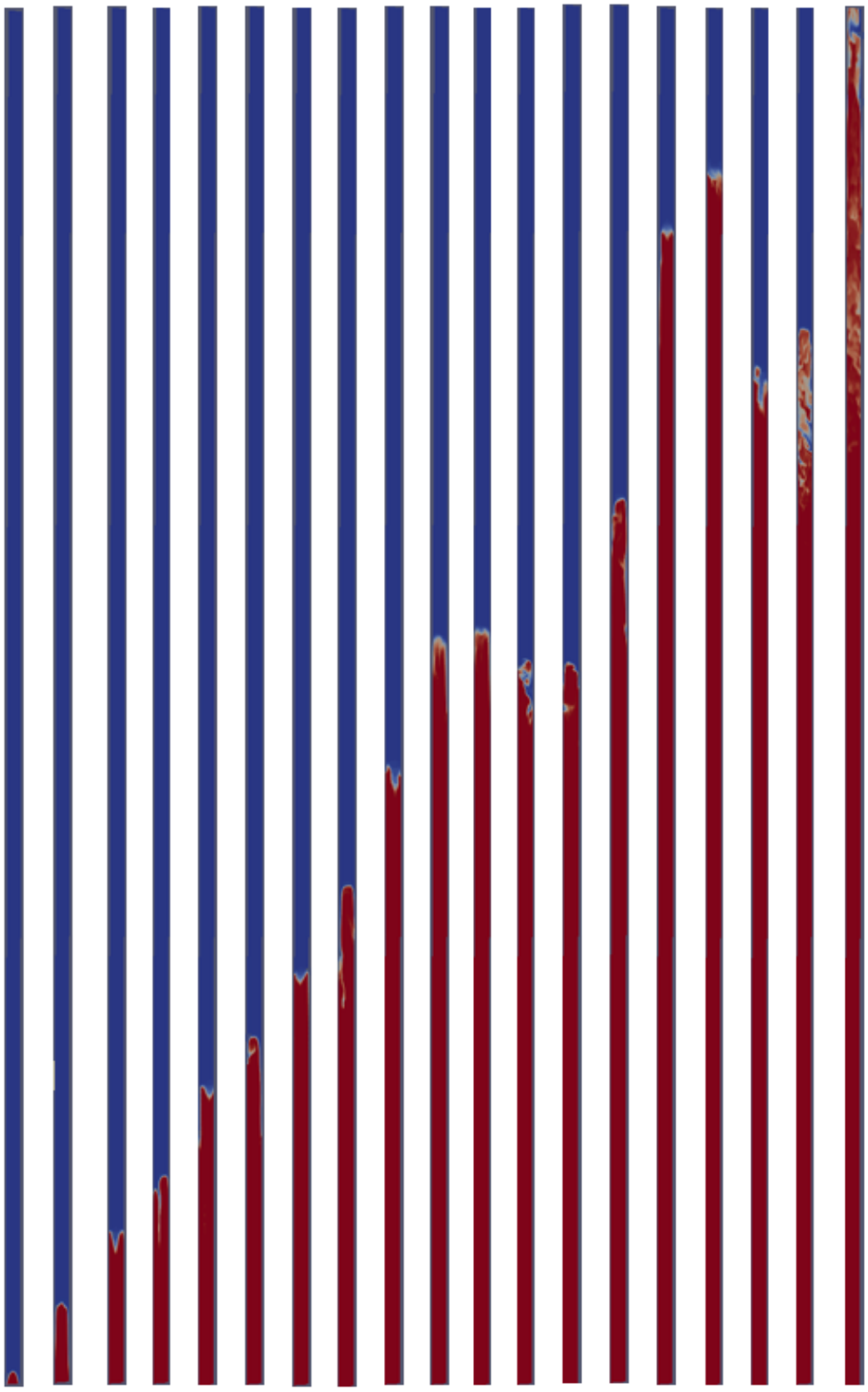

Figure 3: Fields of progress variable (blue: fresh gases, red: burnt gases) ranging from 50 to 950 ms, every 50 ms.

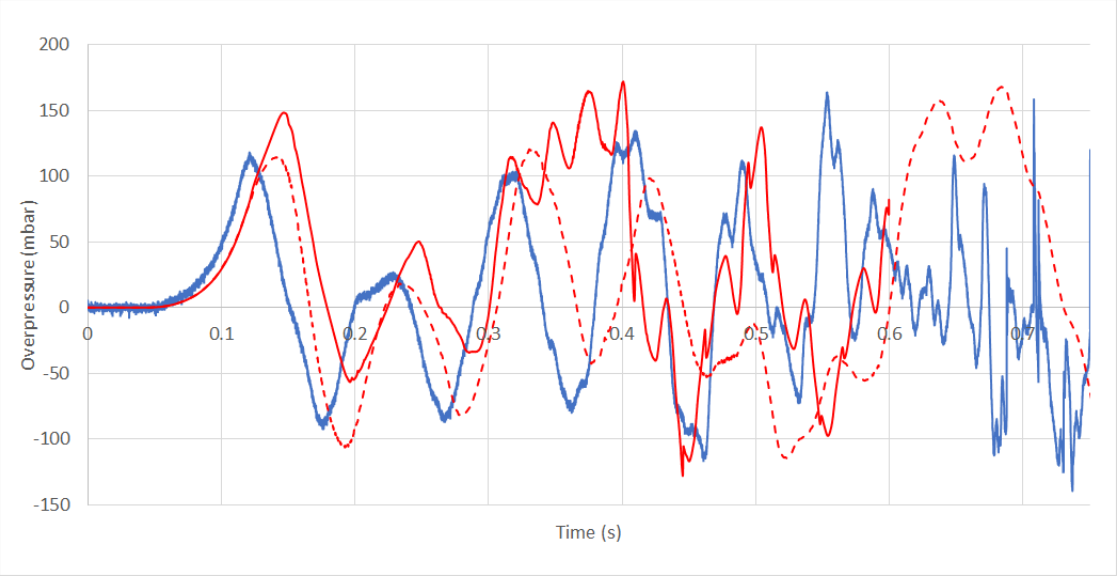

Figure 4: Overpressure signals 15.5 m from ignition point. Case of the 250-mm PPMA pipe. Data from the video post-processing (blue), the computations with (red straight line) and without (red dotted line) a modelled turbulence.

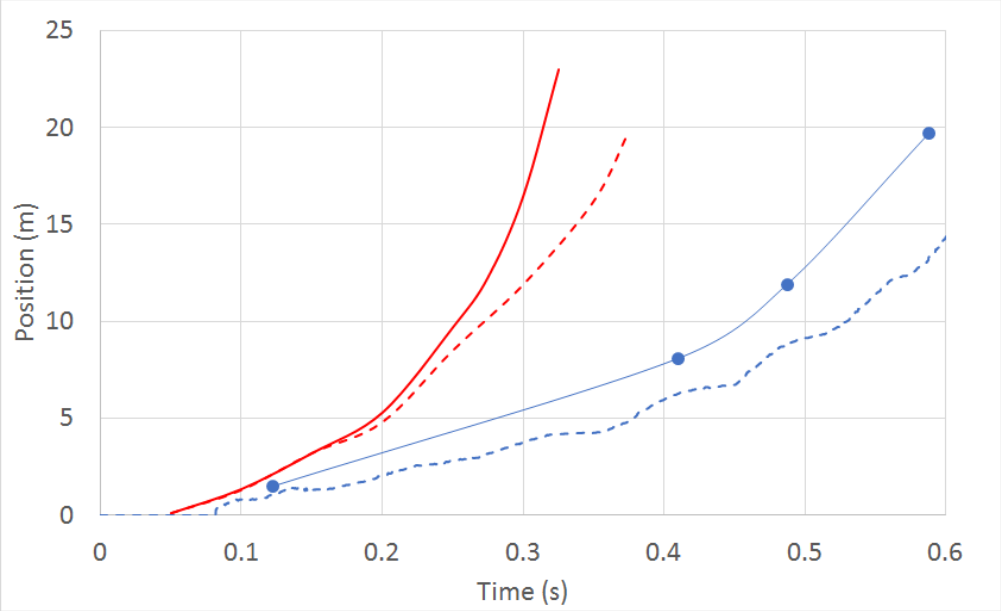

Figure 5: History of the flame front position measured experimentally (blue) and computed with a modelled turbulence (red). Line: metal pipe. Dotted line: PMMA pipe.

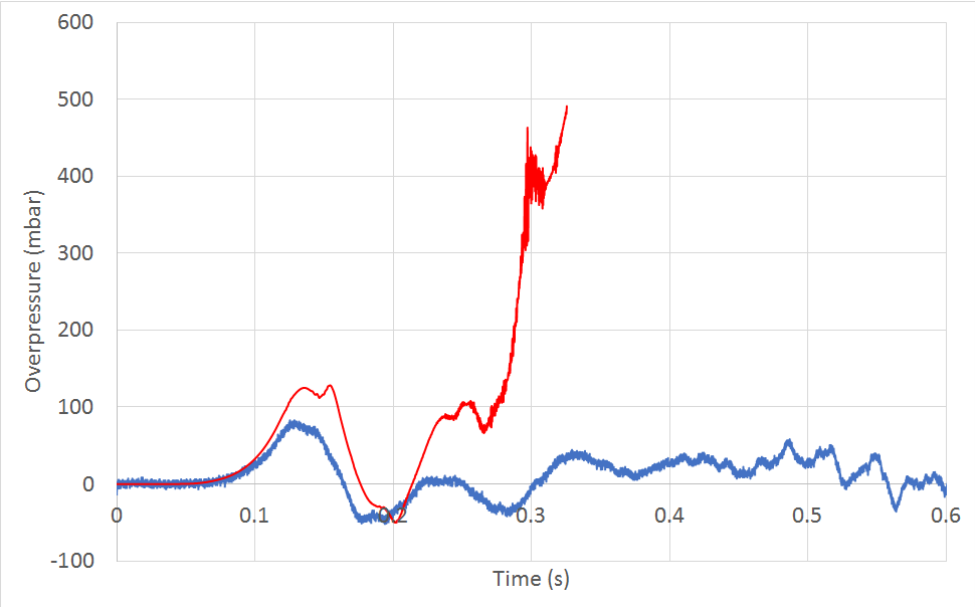

Figure 6: Overpressure signals 15.8 m from ignition point. Case of the 250-mm metal pipe. Data from the video post-processing (blue) and the computation (red).

4.2 150-mm pipes

4.2.1 The PMMA pipe

150 mm pipes are studied to check if the pipe diameter impact on the flame dynamics could be recovered numerically.

For the PMMA pipe, again, two types of models are employed: one with a modelled turbulence, the other with a "laminar" assumption. The position versus time diagram shows (Figure 7) that both models exhibit the same average flame speed from 0 to 0.7 s with oscillations having the same order of magnitude. This observation is somewhat different from the computation results for the 250-mm PMMA pipe with very different histories if the turbulence is modelled or not. Note it is not possible to compare these results with an experimental diagnostic as several camera positions were tested, giving different reconstructed flame histories.

The experimental overpressure signal (Figure 8) is again best approached by the laminar assumption, in terms of characteristic periods and peaks order of magnitude from 0 to 0.3 s. There is nevertheless a time-shift as it appears probable the numerical laminar flame propagates quicker than the experimental flame. As noticed for the 250-mm PMMA pipe, even if the turbulent flame is well too quick, correct orders of magnitude are predicted for the overpressure peaks.

4.2.2 The metal pipe

The metal pipe is modelled with the turbulent flame model accounting for roughness effects at the walls. Figure 9 highlights a good agreement between the experimental and numerical

flame position histories. It can be seen the numerical flame accelerates too strongly compared with the experiments at 0.15 s.

The consequences of these observations on the overpressure signals are shown in Figure 10: the agreement is good as well with pressure history from 0 to 0.2 s but after 0.2 s, the strong acceleration of the numerical flame induces a maximum peak overpressure that about twice the experimental one.

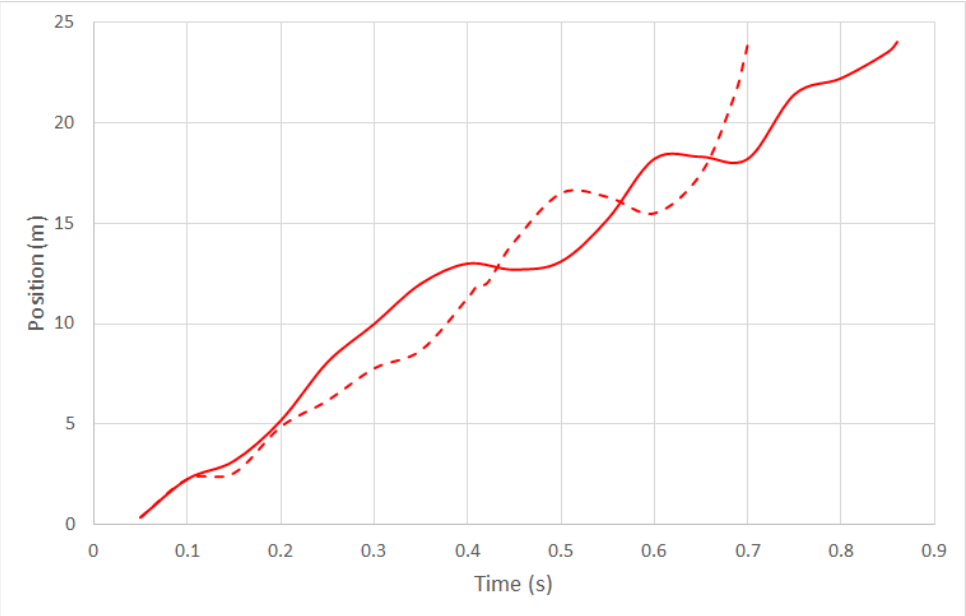

Figure 7: History of the computed flame front position with (line) and without (dotted line) turbulence modelled. Case of the 150-mm PMMA pipe.

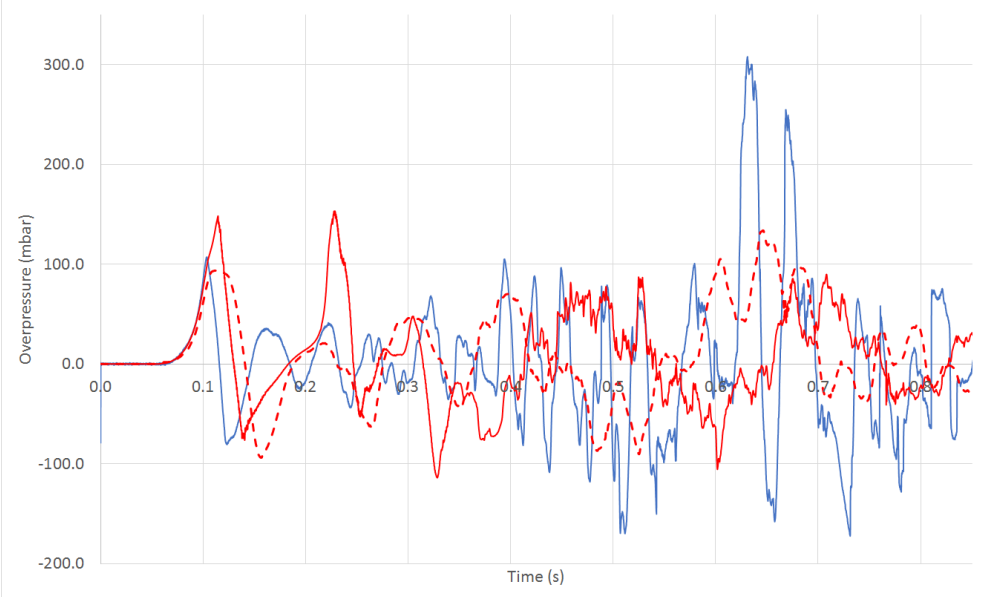

Figure 8: Overpressure signals 15.5 m from ignition point. Case of the 150-mm PMMA pipe. Data from the video post-processing (blue), the computations with (red straight line) and without (red dotted line) a modelled turbulence.

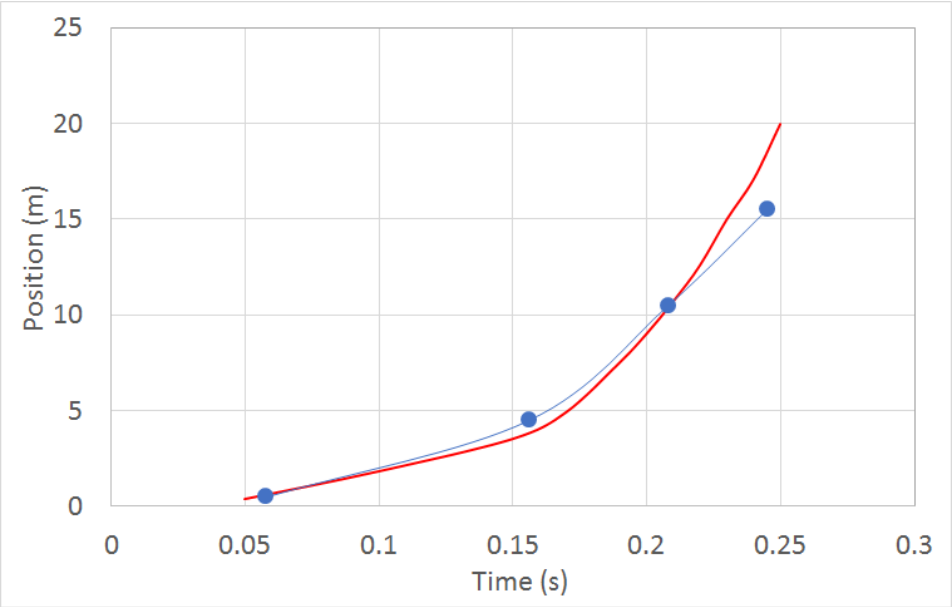

Figure 9: History of the flame front position measured experimentally (blue) and computed (red). Case of the 150-mm metal pipe.

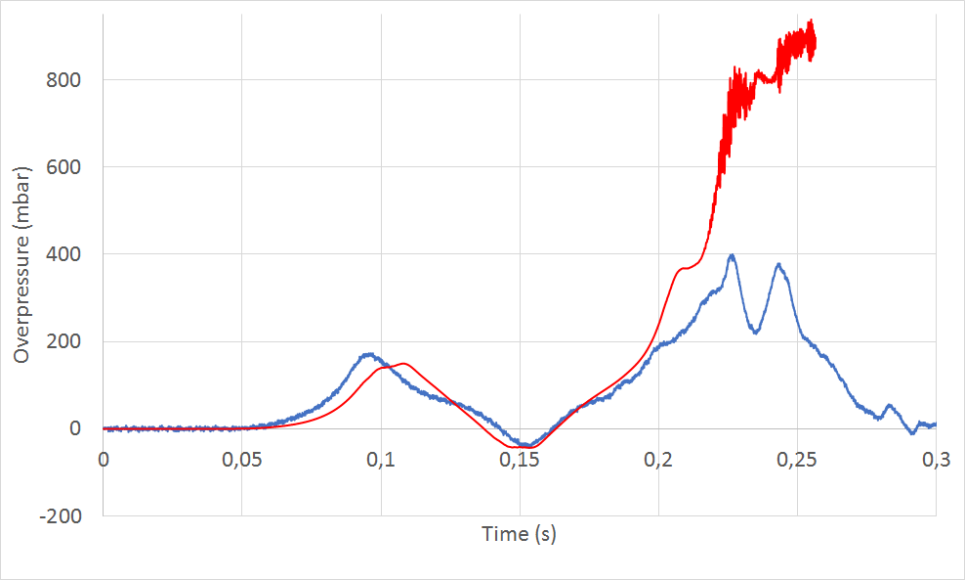

Figure 10: Overpressure signals 15.5 m from ignition point. Case of the 150-mm metal pipe. Data from the photovoltaic cells (blue) and the computations(red).

5. Conclusions

CFD computations were carried out for a set of 24-m long pipes in which initially quiescent, stoichiometric methane/air mixtures are ignited.

The set of compressible equations describing combustion and solving the acoustics was numerically solved with OpenFoam 3.0.0 for four kinds of pipes, with varying materials and diameters.

Even if the numerical results do not perfectly match the experimental measurements and some modelling aspects such as chemistry and the interaction of pressure waves with the atmosphere should be improved, they enable to give first answers to the following questions:

- *It is possible to recover with CFD the experimental flame speed history and pressure signals for such cases?* The results show the capacity of CFD to recover many trends of the phenomena related to premixed flame propagation in pipes: flame shape changes, flame/acoustics coupling, flame acceleration related to rough walls, …
- *What could be the accuracy of CFD*? Orders of magnitude for the pressure peaks were most of the time recovered. Acceleration may be under/overestimated due to the turbulence model and/or the modelling of turbulence at walls. Maybe better results could be obtained with a maximum y^+ value well lower than 200.
- *What is the price to pay by the modeller for getting accurate results? A higher resolution of the physics by the grid, implying more computational power? Or proper modelling choices for turbulence and/or combustion among the bibliography?* The URANS approach could give better results with another turbulence model as the k-ω SST model is known to produce too much turbulence for accelerating flows but it was not checked in this work. An important point is when the flame accelerates, maximum y^+ values increase ahead of the flame front requiring a finer mesh at the walls to limit this increase. For the author, the grid fineness constraint in the model is related to wall treatment. This constraint would be even more demanding for fuels prone to lead to higher flame speed such as hydrogen. The obtained URANS meshes could be compatible with the LES technique but this also should be checked.

Acknowledgements

The authors gratefully acknowledge the financial contribution granted by the Research Fund for Coal and Steel (RFCS) for the EXPRO project during which the presented computations were performed.

References

Daubech, J., Proust Ch., Leprette E. & Lecocq G. (2018). *Further insight into the gas flame acceleration in pipes. Part I: experimental work*. International Symposium on Hazard, Prevention and Mitigation of Industrial Explosions, 12 (submitted).

Guénoche H. (1964). *Nonsteady flame propagation*. Markstein (Ed.), Pergamon Press.

Kerampran S., Desbordes D. & Veyssière B. (2000). *Study of the Mechanisms of Flame Acceleration in a Pipe of Constant Cross Section*. Combustion Science and Technology, 158: 71-91.

Fachini F.F. & Bauwens L. (2013). *Oscillatory flame propagation: Coupling with the acoustic field*. Proceedings of the Combustion Institute, 34: 2043-2048.

Moureau V., Domingo P. & Vervisch L. (2011). *From Large-Eddy-Simulation to Direct Numerical Simulation of a lean premixed swirl flame: Filtered laminar flame PDF modelling*. Combustion and Flame 158(7): 1340-1357

Cornejo I., Niktrityuk P. and Hayes R.E. (2018). *Multiscale RANS-based of the turbulence decay inside of an automotive catalytic converter*. Chemical Engineering Science, 175: 377-386

Urbano A., Douasbin Q., Selle L., Staffelbach G., Cuenot B., Schmitt T., Ducruix S. & Candel S. (2017). *Study of flame response to tranverse acoustic modes from the LES of a 42-injector rocket engine*. Proceedings of the Combustion Institute, 36: 2633-2639.

Makowka K., Dröske N.C., Von Wolfersdorf J. & Sattelmayer T. (2017). *Hybrid RANS/LES of a supersonic combustor*. Aerospace Science and Technology, 69: 563-573.

Pope S.B. (2004). *Ten questions concerning the large-eddy simulation of turbulent flows.* New Journal of Physics, 6: 35.

Weller H.G. & Tabor G. (1998). *A tensorial approach to computational continuum mechanics using object-oriented techniques*. Computational Physics, 12: 620-631.

Menter F.R., Kuntz M., and Langtry R. (2003). *Ten years of industrial experience with the SST turbulence model*. Proceedings of the international symposium on turbulence, heat and mass transfer, 4: 625–632.

Fouladi K., *Elements of Turbulence Modeling*, NAFEMS World Congress

Lecocq G, Richard S., Colin O. & Vervisch L. (2011). *Hybrid presumed pdf and flame surface density approaches for Large-Eddy Simulation of premixed turbulent combustion Part 1: Formalism and simulation of a quasi-steady burner*, Combustion and Flame 158: 1201-1214

Liu C.C., Shy S.S., Peng M.W. & Dong Y.C. (2012). *High-pressure burning velocities measurements for centrally-ignited premixed methane/air flames interacting with intense near-isotropic turbulence at constant Reynolds numbers*, Combustion and Flame, 159: 2608-2619

Morley C. (2005). *Gaseq*. http://www.gaseq.co.uk/

Xiao H., Makarov D., Sun J. and Molkov V. (2012). *Experimental and numerical investigation of premixed flame propagation with distorted tulip shape in a closed duct*. Combustion and Flame, 159(2) : 1523-1538.